Counteracting Selection Bias in Functional Connectivity Studies of Autism

Benjamin Risk

benjamin.risk@emory.edu

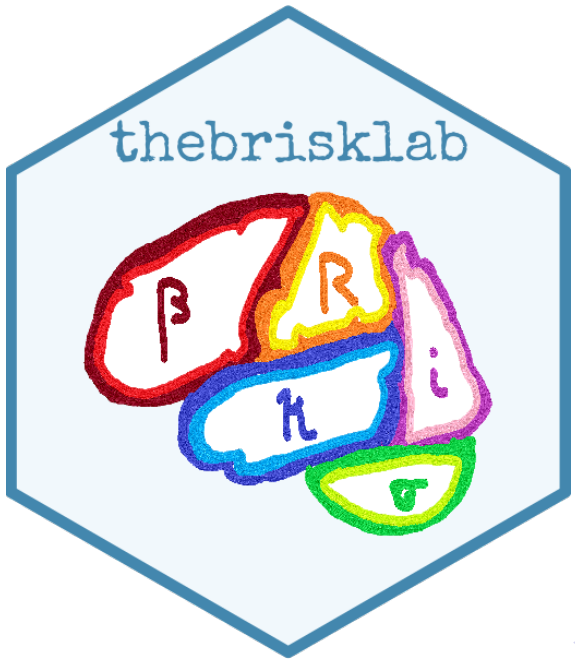

Collaborators

The project team includes students Liangkang Wang, Jialu Ran, Zihang Wang, and Jinyu Wang, and co-investigators David Benkeser, Cheryl Klaiman, Razieh Nabi, Deqiang Qiu, and Sarah Shultz.


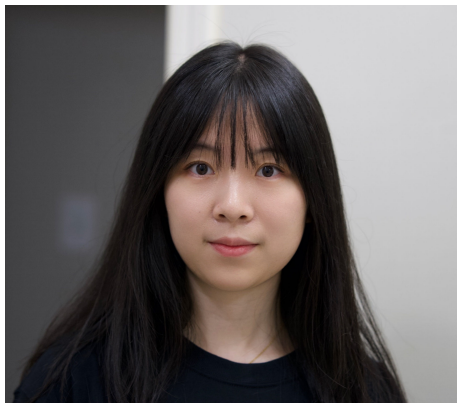

Goal of this talk

- Overview of our approach for accounting for selection bias and improving statistical power in fMRI studies.
- Simulations comparing AIPWE to DRTMLE in smaller sample sizes.
- Propose a computationally scalable permutation test.
- Preliminary results on school-age children in ABIDE.

Motivation: Removal of high motion participants

- Motion in the scanner produces artifacts that are difficult to model (Power et al., 2012).
- Studies recommend excluding "high" motion participants.
- ABCD study with school-aged children removed $60 - 75\%$ of children due to excessive motion (Marek et al., 2022; Nielsen et al., 2019).
- Our previous study found more extensive differences between ASD and TD when using DRTMLE (Nebel et al., 2022), relying upon asymptotic inference.
- In the current study, we focus on methods for smaller sample sizes.
- In current study, we use a more stringent criteria: exclude scans with < 5 min after excluding volumes with mean framewise displacement $> .2$ mm (Power et al., 2014). Hereafter, **Powerpt2**.

School-age children data set

- Autism spectrum disorder is a neurodevelopmental disorder characterized by challenges in social interactions, communication, and repetitive behaviors.
- We are interested in school-aged children (8-13 year-olds) as this is an important age group.
- We selected school-age children from the ABIDE I and II datasets, focusing on the two sites that had > 50 school-age children.

Demographic Table for the Current Study

	TD (N=252)	ASD (N=144)	Total (N=396)	p value
Age				0.680
Mean (SD)	10.400 (1.347)	10.338 (1.594)	10.378 (1.440)	
Range	8.010 - 13.720	8.014 - 13.950	8.010 - 13.950	
Gender				0.003
Male	174 (69.0%)	119 (82.6%)	293 (74.0%)	
Female	78 (31.0%)	25 (17.4%)	103 (26.0%)	
FIQ				< 0.001
Mean (SD)	114.627 (11.507)	103.625 (17.477)	110.626 (14.926)	
Range	80.000 - 144.000	63.000 - 148.000	63.000 - 148.000	
Handedness				0.289
Right	235 (93.3%)	130 (90.3%)	365 (92.2%)	
Left	17 (6.7%)	14 (9.7%)	31 (7.8%)	
ADOS				< 0.001
Mean (SD)	0.000 (0.000)	13.403 (5.245)	4.874 (7.186)	
Range	0.000 - 0.000	6.000 - 35.000	0.000 - 35.000	
Currently on Stimulants				< 0.001
No	252 (100.0%)	116 (80.6%)	368 (92.9%)	
Yes	0 (0.0%)	28 (19.4%)	28 (7.1%)	
Currently on NonStimulants				< 0.001
No	251 (99.6%)	118 (81.9%)	369 (93.2%)	
Yes	1 (0.4%)	26 (18.1%)	27 (6.8%)	
Site ID				< 0.001
ABIDEI-KKI	33 (13.1%)	22 (15.3%)	55 (13.9%)	
ABIDEI-NYU	44 (17.5%)	43 (29.9%)	87 (22.0%)	
ABIDEII-KKI_1	155 (61.5%)	56 (38.9%)	211 (53.3%)	
ABIDEII-NYU_1	20 (7.9%)	23 (16.0%)	43 (10.9%)	
ciric				< 0.001
Unusable	39 (15.5%)	45 (31.2%)	84 (21.2%)	
Usable	213 (84.5%)	99 (68.8%)	312 (78.8%)	
powerpt2				< 0.001
Unusable	126 (50.0%)	110 (76.4%)	236 (59.6%)	
Usable	126 (50.0%)	34 (23.6%)	160 (40.4%)	

Table: **Socio-demographic characteristics**

Motion distributions in ASD and TD children

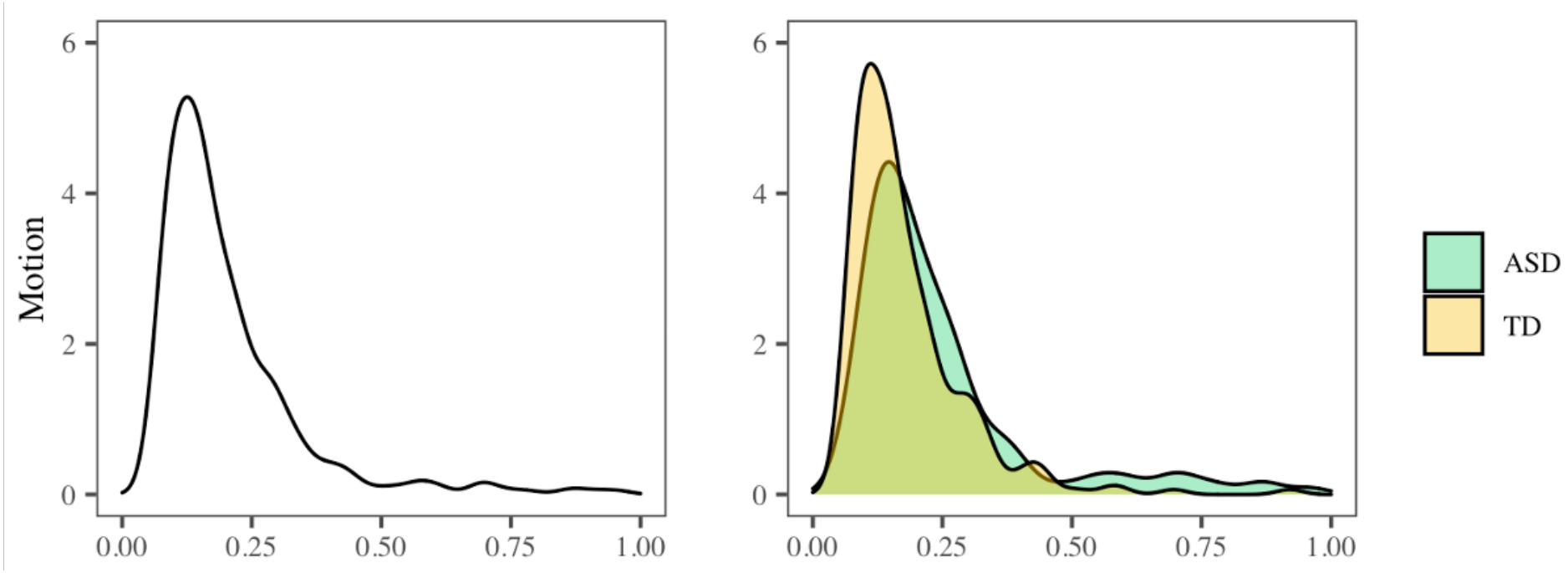

Figure: Mean FD (mm). Children move a lot. Autistic children move even more.

Selection bias

- $Y(\Delta = 1)$, i.e., $Y(1)$, is the counterfactual that a participant's scan is usable. Define associational parameter (Nebel et al., 2022):

$$\begin{aligned}\psi^* &= E^*[Y(1)|A=1] - E^*[Y(1)|A=0] \\ &= E^*\left\{E^*\left(Y(1)|A=1,W\right)|\, A=1\right\} \\ &\quad - E^*\left\{E^*\left(Y(1)|A=0,W\right)|A=0\right\}.\end{aligned}$$

- $\psi_{naive} = E[Y|\Delta=1, A=1] - E[Y|\Delta=1, A=0]$.
- Define selection bias: $\psi_{naive} \neq \psi^*$.
- Confounding bias and selection bias: concepts overlap; see (Hernan and Robins, 2020) p. 80 for detailed discussion.
- Key: lack of exchangeability between usable and unusable data.
- Bias can arise when $\Delta \leftrightarrow W$, $W \leftrightarrow Y$. Then $E^*[Y(1)|A=1] \neq E[Y|\Delta=1, A=1]$

Target Parameter and Identifiability Assumptions

- Define our target parameter, the debiased group difference:

$$\psi = E\{E(Y \mid \Delta = 1, A = 1, W) \mid A = 1\} - E\{E(Y \mid \Delta = 1, A = 0, W) \mid A = 0\}.$$

- Identifiability assumptions: $\psi^* = \psi$ if
  - (A1.1) *Mean exchangeability (no missing confounders)*: for $a = 0, 1$, $E^*\{Y(1) \mid A = a, W\} = E^*\{Y(1) \mid \Delta = 1, A = a, W\}$.
  - (A1.2) *Positivity*: for $a = 0,\ 1$ and all possible w, $P(\Delta = 1 \mid A = a, W = w) > 0$.
  - (A1.3) *Causal Consistency*: for all i such that $\Delta_i = 1$, $Y_i(1) = Y_i$.

Notation

Notation:

- Let n_1 be the number of children with ASD
- $\{i \in \mathcal{S}_1\}$ denote the set of indices for ASD children.
- Similarly, define n_0 and $\{i \in \mathcal{S}_0\}$ for the TD children.

IPWE and G-Comp

- Inverse probability weighted estimator:
  - Use **ensemble of machine learning methods** to fit propensity model: $\hat{p}(A_i, W_i)$.
  - Inverse probability weighted estimator for correlation between DMN seed region and **regions $j = 1, \ldots, 400$**:

$$\hat{\psi}_{j,IPWE} = \frac{1}{n_1} \sum_{i \in \mathcal{S}_1} \left(\frac{\Delta_i}{\hat{p}(A_i, W_i)} Y_{ij} \right) - \frac{1}{n_0} \sum_{i \in \mathcal{S}_0} \left(\frac{\Delta_i}{\hat{p}(A_i, W_i)} Y_{ij} \right).$$

- G-Computation estimator:
  - Fit outcome model with **superlearner** (Van Der Laan et al., 2007):

$$\hat{Y}_{ij} = \bar{Q}_j(A_i, W_i).$$

  - Predict values for all i (usable and unusable):

$$\hat{\psi}_{j,GComp} = \frac{1}{n_1} \sum_{i \in \mathcal{S}_1} \hat{Y}_{ij} - \frac{1}{n_0} \sum_{i \in \mathcal{S}_0} \hat{Y}_{ij}.$$

AIPWE

- The Augmented Inverse Probability Weighted Estimator combines IPWE and G-Computation in missing data (Bang and Robins, 2005):

$$\hat{\psi}_{j,AIPWE} = \frac{1}{n_1} \sum_{i \in \mathcal{S}_1} \left(\left[\frac{I(\Delta_i = 1)}{\hat{p}(A_i, W_i)} \right] Y_{ij} + \left[1 - \frac{I(\Delta_i = 1)}{\hat{p}(A_i, W_i)} \right] \bar{Q}_j(A_i, W_i) \right)$$
$$- \frac{1}{n_0} \sum_{i \in \mathcal{S}_0} \left(\left[\frac{I(\Delta_i = 1)}{\hat{p}(A_i, W_i)} \right] Y_{ij} + \left[1 - \frac{I(\Delta_i = 1)}{\hat{p}(A_i, W_i)} \right] \bar{Q}_j(A_i, W_i) \right).$$

- Doubly robust estimate of mean: if either propensity or outcome model is correct, consistent estimator.
- Standard errors are not consistent if model mis-specified (but we will use superlearner to flexibly model propensity and outcome models).

Doubly robust targeted minimum loss based estimation

- Benkeser et al. (2017) developed a doubly robust targeted minimum loss-based estimator: if *at least* one of the two regressions is consistently estimated, both $\hat{\psi}$ *and its SE* are consistently estimated.

1. Fit propensity model.
2. Fit outcome model.
3. Apply DRTMLE to propensities and predicted outcomes. Involves a special iterative logistic regression.
4. Great theoretical properties – use when you have thousands of participants.

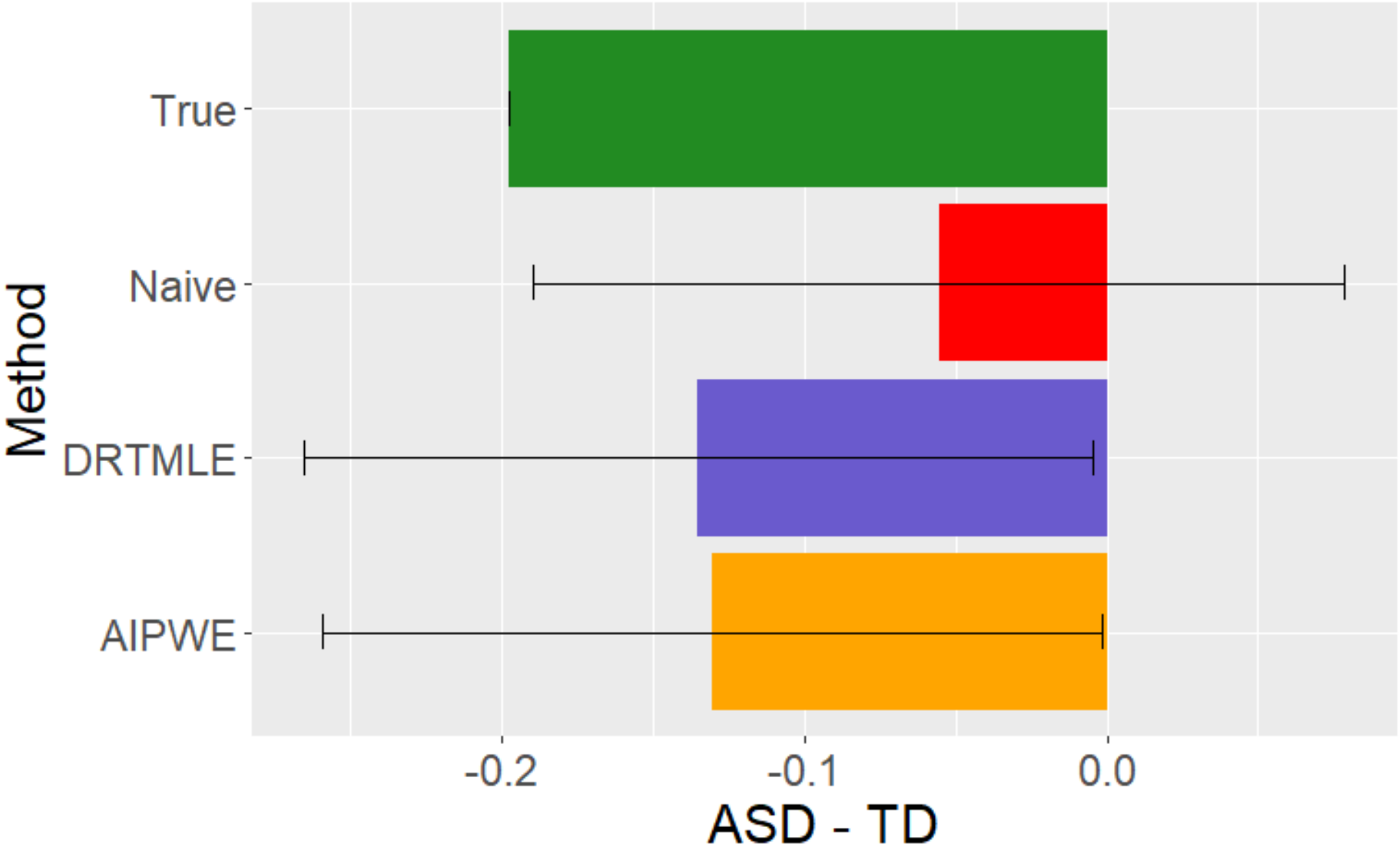

Figure: **Estimate of functional connectivity from DRTMLE and AIPWE compared to naive data removal from a toy simulation.**

Perm Tests and Computational considerations

- Permutation tests are popular for finite-sample inference in neuroimaging.
- The propensity and outcome models require fitting superlearner with 10-fold CV for propensity and outcome models: `SL.earth`, `SL.glmnet`, `SL.gam`, `SL.glm`, `SL.ranger`, `SL.ridge`, `SL.step`, `SL.step.interaction`, `SL.svm`, `SL.xgboost`.
- CV is sensitive to random seed, fit 20 times for propensity model, average $\hat{p}(A_i, W_i)$, fit 20 times for each of 400 locations, average $\bar{Q}_j(A_i, W_i)$.
- Involves fitting regressions to approximately 400 locations with 20 random seeds and 10 learners and 10-fold CV $\approx$ 800,000.

Novel Permutation test

- Computationally scalable: permute membership of $\mathcal{S}_1$ and $\mathcal{S}_0$, call $\mathcal{S}_1^{(k)}$ and $\mathcal{S}_0^{(k)}$.

$$\hat{\psi}_{j,AIPWE}^{(k)} = \frac{1}{n_1} \sum_{i \in \mathcal{S}_1^{(k)}} \left(\left[\frac{I(\Delta_i = 1)}{\hat{p}(A_i, W_i)} \right] Y_{ij} + \left[1 - \frac{I(\Delta_i = 1)}{\hat{p}(A_i, W_i)} \right] \bar{Q}_j(A_i, W_i) \right)$$
$$- \frac{1}{n_0} \sum_{i \in \mathcal{S}_0^{(k)}} \left(\left[\frac{I(\Delta_i = 1)}{\hat{p}(A_i, W_i)} \right] Y_{ij} + \left[1 - \frac{I(\Delta_i = 1)}{\hat{p}(A_i, W_i)} \right] \bar{Q}_j(A_i, W_i) \right)$$

- Standardize by asymptotic standard error to generate z_j.
- **Family-wise error rate control**:

$$p_{j,fwer} = \frac{1}{K} \sum_{k=1}^{K} I \left(\left\{ \max_j |z_j^{(k)}| \right\} > |z_j| \right)$$

Novel Permutation test

- Under the null hypothesis,

$$E\{E(Y_j \mid \Delta = 1, A = 1, W) \mid A = 1\}$$
$$-E\{E(Y_j \mid \Delta = 1, A = 0, W) \mid A = 0\} = 0.$$

- In the permutation test, we preserve the inner conditional expectation, $E(Y_j \mid \Delta = 1, A, W)$ by using the estimates

$$\left[\frac{I(\Delta_i = 1)}{\hat{p}(A_i, W_i)}\right] Y_{ij} + \left[1 - \frac{I(\Delta_i = 1)}{\hat{p}(A_i, W_i)}\right] \bar{Q}_j(A_i, W_i)$$

.

- We obtain a null distribution for our finite sample since

$$E\hat{\psi}^{(k)}_{j,AIPWE} = E\{E(Y_j \mid \Delta = 1, A = 1, W)\}$$
$$-E\{E(Y_j \mid \Delta = 1, A = 0, W)\}.$$

Simulations: strong correlation

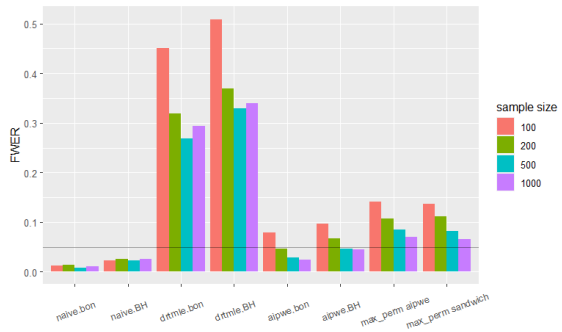

(a) FWER from 81 regions

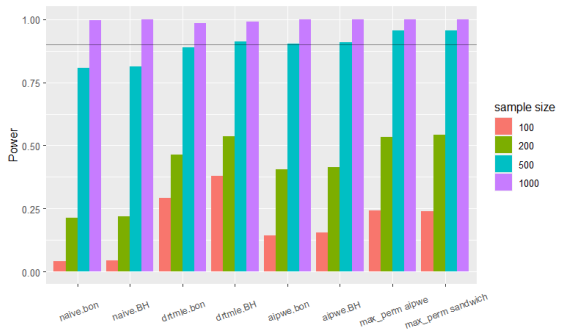

(b) Power

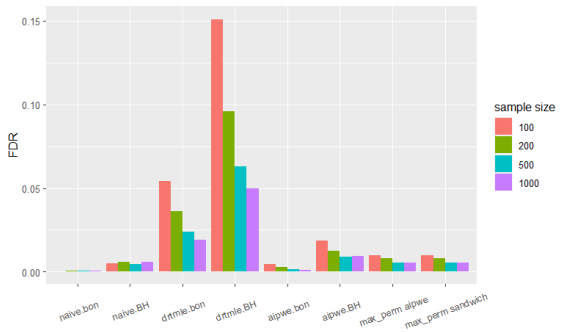

(c) FDR for 81 regions

Figure: Simulation setting 2 (within-block correlation = 0.9, three blocks, 81 regions). a) Inflated FWER in permutation test may be due to exchangeability violations.

Simulations: data-based correlation

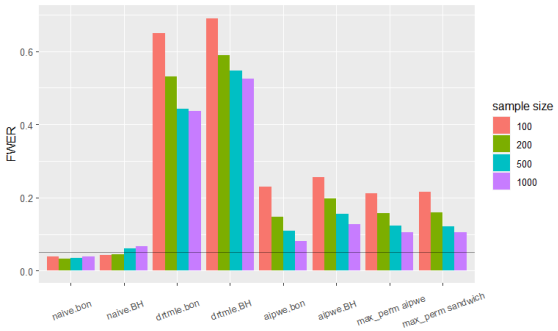

(a) FWER from 81 regions

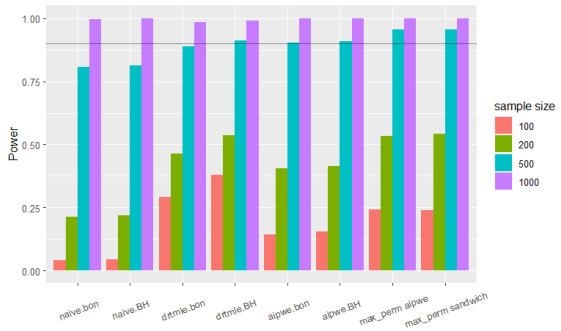

(b) Power

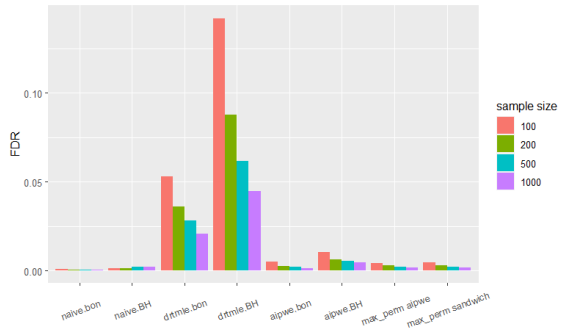

(c) FDR for 81 regions

Figure: Simulation setting 3 (data-based correlation between errors across 81 regions).

Simulations summary

- AIPWE has fewer false positives than DRTMLE – the improved (asymptotic) robustness in DRTMLE comes at a cost for $n < 1000$.
- AIPWE has improved power for naive removal of scans.
- Max perm didn't show many benefits over AIPWE. Some power gains but mixed results with type 1 errors.
- Adequate FDR control for AIPWE, still problems with FWER control in some settings.

Previous study: motion exclusion criteria in functional MRI can cause sampling bias

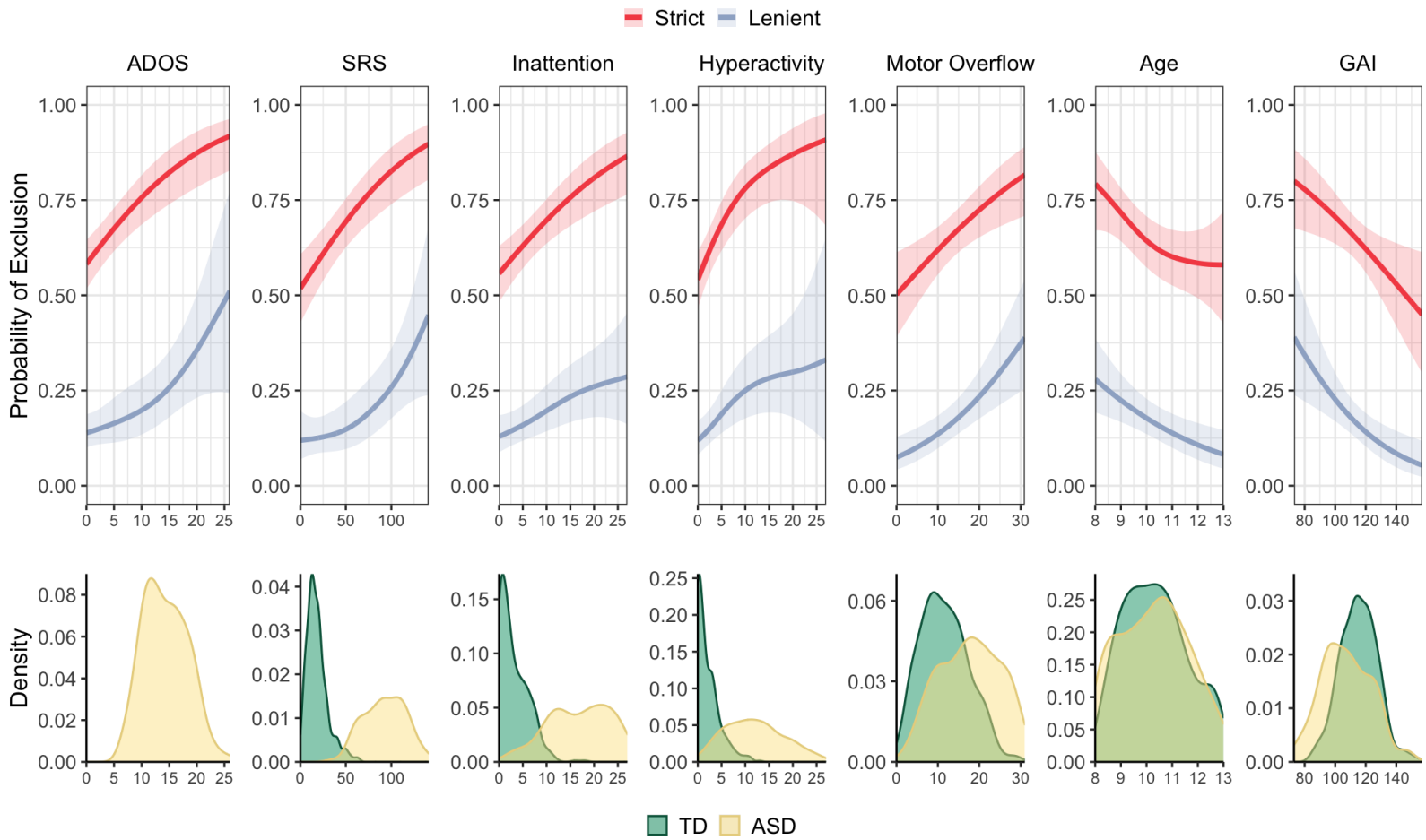

Figure: From Nebel et al. (2022).

Current study: no relationship between motion exclusion criteria and ADOS, Age, or FIQ

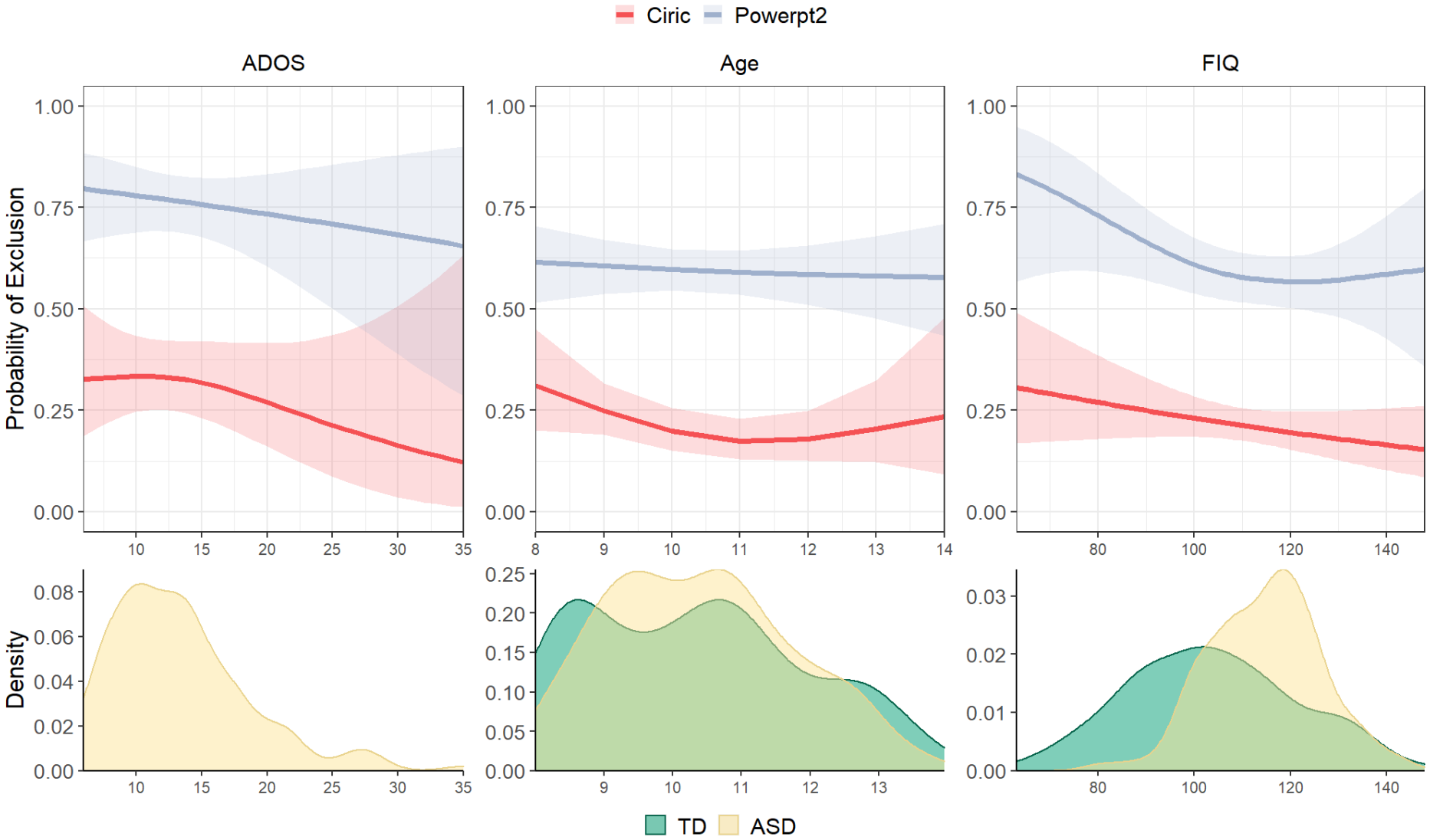

Resting-state fMRI analysis

- We performed preprocessing using fmriprep with `--cifti-output`.
- Visually inspected segmentation, 17 had issues.
- Used 400-node parcellation from (Schaefer et al., 2018) and `ciftiTools` following the tutorial in (Pham et al., 2022).
- Used a region in the default mode network as a seed region and focused on its correlation with 399 regions, since DMN is thought to be important in ASD (Di Martino et al., 2014).
- COMBAT for siteXacquisitionXheadcoil harmonization (Fortin et al., 2017).
- Use **ensemble of machine learning methods** (Van Der Laan et al., 2007) to fit the outcome and propensity models using the variables: diagnosis, ADOS, FIQ, stimulants, non-stimulants, age, sex, and handedness.

QC of school-age children in ABIDE I and II

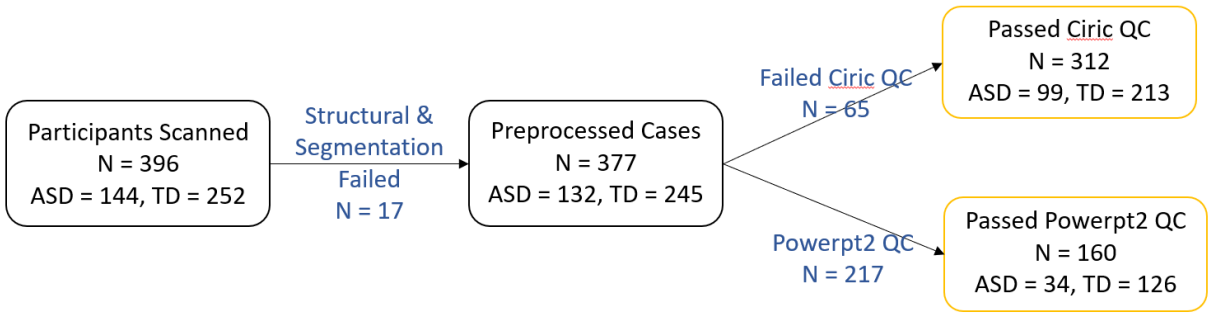

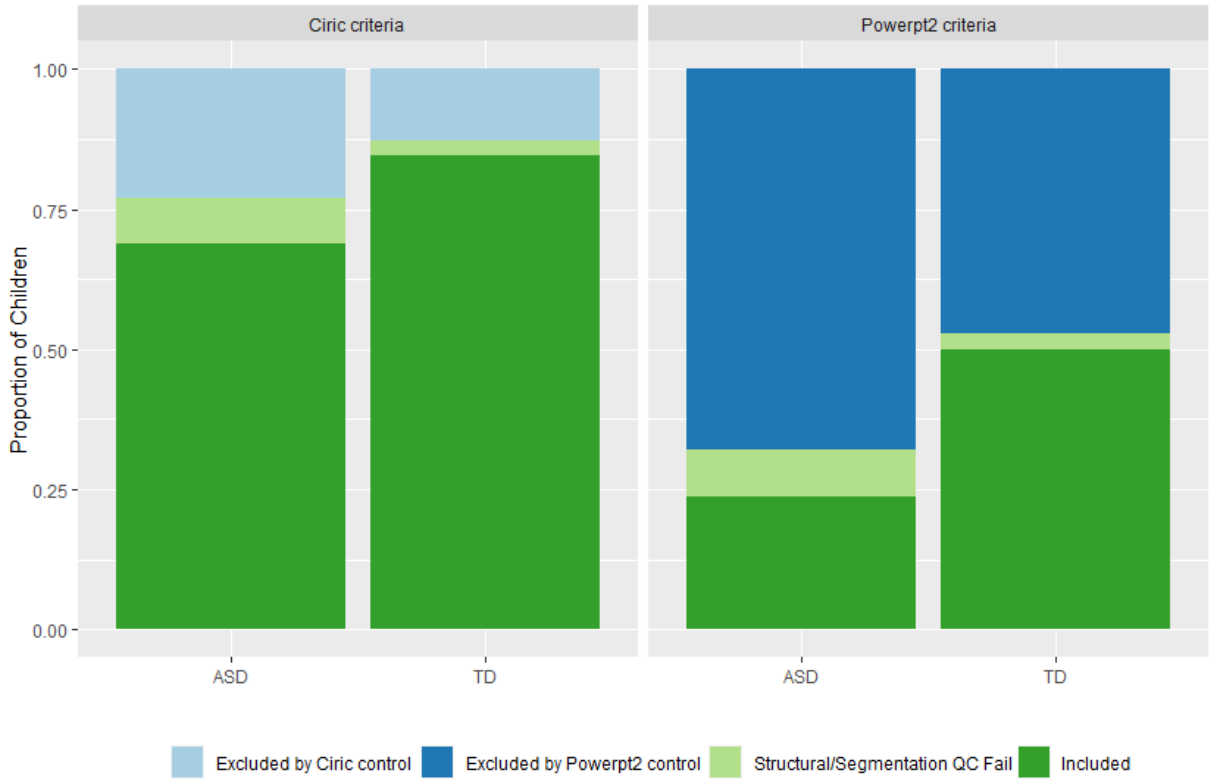

Preliminary results: Naive versus AIPWE

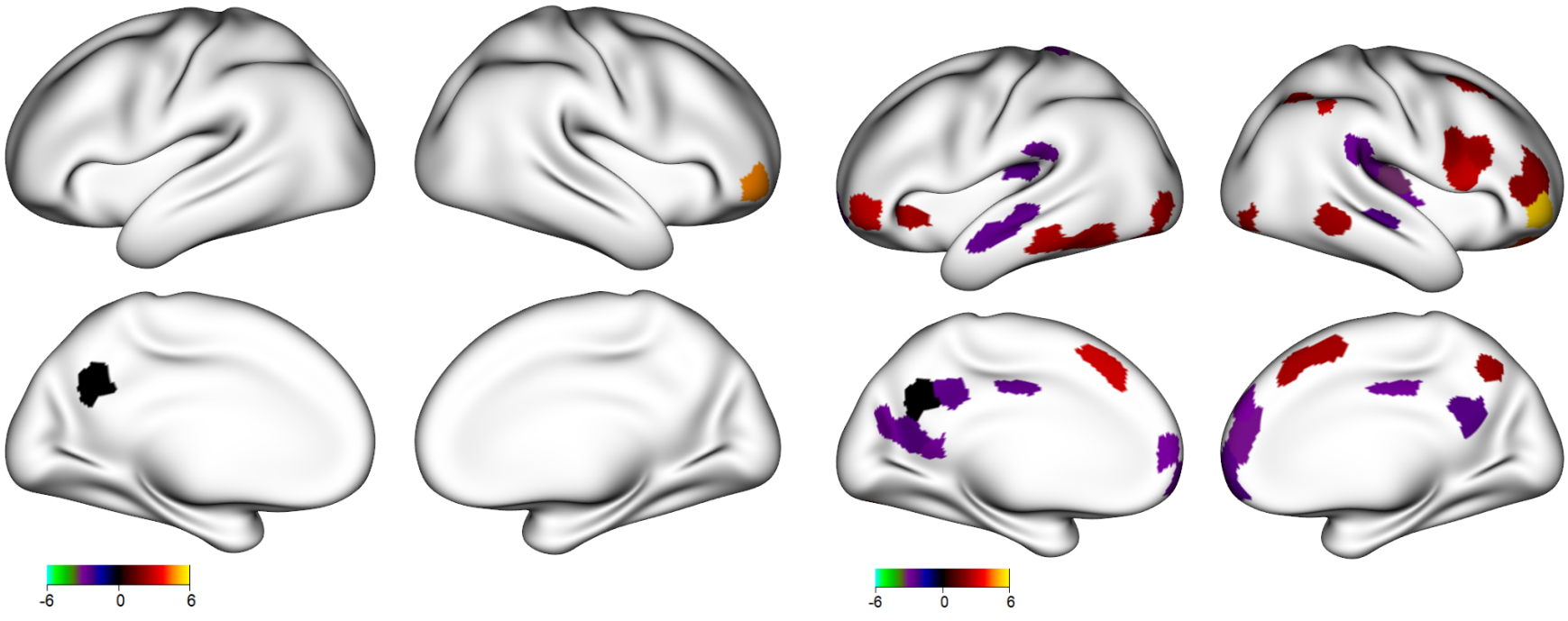

(a) Naive FDR=0.20

(b) AIPWE FDR=0.20

Figure: Z-stats from naive removal of high motion scans versus AIPWE. $ASD - TD$, thresholded at FDR=0.20. At FDR=0.05, 1 region in Naive, 2 regions in AIPWE.

Returning to our goals

- Overview of our approach for accounting for selection bias and improving statistical power in fMRI studies.

  DRTMLE and AIPWE can reduce sample bias and improve power.

- Compare AIPWE to DRTMLE in smaller sample sizes.

  In simulations, AIPWE had better type-1 error control, but still inflated in some settings.

- Propose a computationally scalable permutation test.

  Results are mixed.

- Results on school-age children from Autism Brain Imaging Data Exchange.

  With 34 usable scans from Autistic children, we found evidence of differences between ASD and TD children using AIPWE.

Limitations

- Additional research to disentangle false positives from true positives.
- Preliminary results using bootstraps are promising, working on computational scalability.
- Examine other applications where we expect selection bias – ABCD developmental differences between boys and girls, cortical thickness studies in Alzheimer's, ADHD, prospective Autism study in the brisklab with richer phenotyping.

Acknowledgments

This research was supported by the National Institute of Mental Health of the National Institutes of Health under award number R01 MH129855. The content is solely the responsibility of the authors and does not necessarily represent the official views of the National Institutes of Health.

Thank you!

- Thank you!
- https://github.com/thebrisklab
- We are looking for a post doc or research scientist: email benjamin.risk@emory.edu.

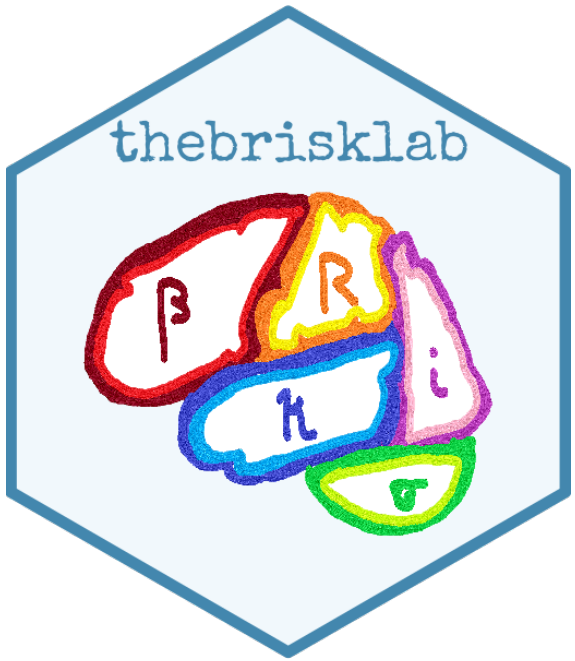

References I

Bang, H. and Robins, J. M. (2005). Doubly Robust Estimation in Missing Data and Causal Inference Models. *Biometrics*, 61(4):962–973.

Benkeser, D., Carone, M., Laan, M. J. V. D., and Gilbert, P. B. (2017). Doubly robust nonparametric inference on the average treatment effect. *Biometrika*, 104(4):863–880.

Di Martino, A., Yan, C.-G., Li, Q., Denio, E., Castellanos, F. X., Alaerts, K., Anderson, J. S., Assaf, M., Bookheimer, S. Y., Dapretto, M., Deen, B., Delmonte, S., Dinstein, I., Ertl-Wagner, B., Fair, D. A., Gallagher, L., Kennedy, D. P., Keown, C. L., Keysers, C., Lainhart, J. E., Lord, C., Luna, B., Menon, V., Minshew, N. J., Monk, C. S., Mueller, S., Müller, R.-A., Nebel, M. B., Nigg, J. T., O'Hearn, K., Pelphrey, K. A., Peltier, S. J., Rudie, J. D., Sunaert, S., Thioux, M., Tyszka, J. M., Uddin, L. Q., Verhoeven, J. S., Wenderoth, N., Wiggins, J. L., Mostofsky, S. H., and Milham, M. P. (2014). The autism brain imaging data exchange: towards a large-scale evaluation of the intrinsic brain architecture in autism. *Mol. Psychiatry*, 19(6):659–667.

References II

Fortin, J.-P., Parker, D., Tunç, B., Watanabe, T., Elliott, M. A., Ruparel, K., Roalf, D. R., Satterthwaite, T. D., Gur, R. C., Gur, R. E., Schultz, R. T., Verma, R., and Shinohara, R. T. (2017). Harmonization of multi-site diffusion tensor imaging data. *Neuroimage*, 161:149–170.

Hernan, M. and Robins, J. (2020). *Causal Inference: What If*. Chapman Hall/CRC, Boca Raton.

Marek, S., Tervo-Clemmens, B., Calabro, F. J., Montez, D. F., Kay, B. P., Hatoum, A. S., Donohue, M. R., Foran, W., Miller, R. L., Hendrickson, T. J., Malone, S. M., Kandala, S., Feczko, E., Miranda-Dominguez, O., Graham, A. M., Earl, E. A., Perrone, A. J., Cordova, M., Doyle, O., Moore, L. A., Conan, G. M., Uriarte, J., Snider, K., Lynch, B. J., Wilgenbusch, J. C., Pengo, T., Tam, A., Chen, J., Newbold, D. J., Zheng, A., Seider, N. A., Van, A. N., Metoki, A., Chauvin, R. J., Laumann, T. O., Greene, D. J., Petersen, S. E., Garavan, H., Thompson, W. K., Nichols, T. E., Yeo, B. T., Barch, D. M., Luna, B., Fair, D. A., and Dosenbach, N. U. (2022). Reproducible brain-wide association studies require thousands of individuals. *Nature 2022 603:7902*, 603(7902):654–660.

References III

Nebel, M. B., Lidstone, D. E., Wang, L., Benkeser, D., Mostofsky, S. H., and Risk, B. B. (2022). Accounting for motion in resting-state fMRI: What part of the spectrum are we characterizing in autism spectrum disorder? *NeuroImage*, 257.

Nielsen, A. N., Greene, D. J., Gratton, C., Dosenbach, N. U., Petersen, S. E., and Schlaggar, B. L. (2019). Evaluating the prediction of brain maturity from functional connectivity after motion artifact denoising. *Cerebral Cortex*, 29(6):2455–2469.

Pham, D. D., Muschelli, J., and Mejia, A. F. (2022). ciftitools: A package for reading, writing, visualizing, and manipulating CIFTI files in R. *Neuroimage*, 250(118877):118877.

Power, J. D., Barnes, K. A., Snyder, A. Z., Schlaggar, B. L., and Petersen, S. E. (2012). Spurious but systematic correlations in functional connectivity MRI networks arise from subject motion. *NeuroImage*, 59(3):2142–2154.

Power, J. D., Mitra, A., Laumann, T. O., Snyder, A. Z., Schlaggar, B. L., and Petersen, S. E. (2014). Methods to detect, characterize, and remove motion artifact in resting state fMRI. *NeuroImage*, 84:320–341.

References IV

Schaefer, A., Kong, R., Gordon, E. M., Laumann, T. O., Zuo, X.-N., Holmes, A. J., Eickhoff, S. B., and Yeo, B. T. T. (2018). Local-global parcellation of the human cerebral cortex from intrinsic functional connectivity MRI. *Cereb. Cortex*, 28(9):3095–3114.

Van Der Laan, M. J., Polley, E. C., and Hubbard, A. E. (2007). Super learner. *Statistical Applications in Genetics and Molecular Biology*, 6(1).